ELSEVIER

Physics of the Earth and Planetary Interiors 103 (1997) 365–374

PHYSICS OF THE EARTH AND PLANETARY INTERIORS

Elliptical instability of the Earth's fluid core

Keith Aldridge *, Behnam Seyed-Mahmoud, Gary Henderson, William van Wijngaarden

Centre for Research in Earth and Space Science, York University, 4700 Keele Street, North York, Ontario, Canada

Received 7 February 1997; received in revised form 19 May 1997; accepted 20 May 1997

Abstract

The elliptical instability of a rotating fluid contained in a thick spherical shell has been excited in our laboratory by a tide-like perturbation of the flexible inner boundary. For an inviscid fluid, the growth rate of the instability is approximately proportional to the perturbation amplitude and the rotation rate. Development of the instability appears to be limited by the spherical outer surface and the relatively small perturbation applied over the inner surface. If the corresponding instability were excited in the Earth's fluid core by tidal forces, in the absence of dissipation the e-folding time for growth would be on the order of several thousand years. Although this time scale is similar to current estimates for the time needed for the geomagnetic field to undergo a reversal, the instability would grow at a rate equal to the difference between the ideal growth rate and the overall decay rate. The rates of viscous and electromagnetic damping are determined by material properties of the core fluid that are not well known. If elliptical instability plays a central role in geomagnetic reversals, upper limits on the viscosity and conductivity of the fluid core might be inferred. © 1997 Elsevier Science B.V.

Keywords: Earth's fluid core; Tidal forces; Elliptical instability; Geomagnetic reversals

1. Introduction

It is well known that deformation of the circular streamlines of a contained rotating fluid can produce an unstable response whereby an otherwise laminar flow becomes turbulent. For an effectively inviscid fluid, the perturbation may be small enough that only terms up to first order need be considered in the equations of motion to adequately model the response. Indeed, the elliptical type of such instability has been produced in laboratory experiments on fluids contained by cylindrical boundaries with perturbation amplitudes as low as 1% (Vladimirov and Tarasov, 1985; Malkus, 1989). A slight vibration of a rotating fluid about a state with circular streamlines is called an inertial mode, whereas a greater deviation from a state with elliptical streamlines is called an elliptical instability. The deformation from circular to elliptical streamlines is accompanied by a transition from real to complex frequencies, so an inviscid inertial mode only has a frequency but an elliptical instability also has a growth rate. In essence, an elliptical instability consists of inertial modes that have promoted themselves far beyond the classical regime where advection of the fluid particles through the velocity field is negligible in the rotating frame of reference. The signature of an elliptical instability within a fluid contained by a cylindrical boundary is

* Corresponding author.

PII S0031-9201(97)00065-4

a locus of stagnation points as though the rotation axis were bent into a sinusoid. Clearly the velocity scale for the disturbance in the rotating frame of reference is then comparable with that for the rotation in the laboratory frame. Although its frequency and growth rate are predicted by linear theory, a mature elliptical instability is a highly non-linear flow.

Vladimirov and Tarasov (1985) depicts the onset of hydrodynamic instability within a rotating cylinder of elliptical cross-section. The cylinder and fluid were set into solid-body rotation, then the cylinder was stopped so that the fluid moved past the elliptical perturbation, which produced a transient instability seen by means of dye along the axis. Malkus (1989) describes a similar instability that was repeatedly produced within a rotating cylinder whose flexible walls were deformed by a pair of rollers fixed at opposite sides in the laboratory frame of reference. In this experiment the elliptical instability of the fluid was observed to grow, break down, and decay in succession, as long as the tide-like perturbation was applied.

It is now recognized that a so-called 'resonant collapse', as studied in experiments by Thompson (1970) and McEwan (1970), is probably from the same family as the elliptical instability, but of shear type, as described by Kerswell (1993). McEwan (1970) shows the onset of resonant collapse in a rotating cylinder of fluid perturbed by precessing the lid, and Manasseh (1992) reports a similar result in a rotating cylinder of fluid perturbed by precessing the whole. More recently, Manasseh (1994) has interpreted the response of a fluid rotating within a precessing cylinder as the shear instability. A combination of the shear and elliptical instabilities has been observed by Vanyo et al. (1995), who precessed a rotating spheroid and found unstable regions in the contained fluid.

Our interest in the elliptical instability of a rotating fluid dates back to Lumb et al. (1993), where the possibility of its excitation within a spherical shell was suggested. There were two reasons to pursue such an idea: one mathematical and the other geophysical. Mathematically, an elliptical instability owes its existence to a resonance of inertial modes that are represented by solutions of the ill-posed Poincaré problem. The absence of certain inertial modes from the spectrum of a spherical shell would mean the lack of a mechanism for the associated elliptical instability in that geometry. Geophysically, an elliptical instability might be repeatedly excited in the fluid outer core of the Earth by the slight tidal deformation of the core–mantle boundary. If so, the growth of inertial modes into non-linear flows would become central to dynamo theories of the geomagnetic field.

A laboratory experiment would determine whether such an instability could be excited in a thick spherical shell and under what conditions. Fundamental to elliptical instability is the existence of inertial modes with azimuthal wavenumbers of zero, one, and two. Of course, those with the value zero are axially symmetric oscillations, whereas those with the larger values are azimuthally travelling waves. The relevant geometry had been adopted before to excite inertial modes of wavenumber zero (Aldridge, 1975) and wavenumber one (Stergiopoulos and Aldridge, 1984; Lumb and Aldridge, 1988). Thus a real fluid, with a small but finite viscosity, was known to support a number of inertial modes in a rotating spherical shell, and this fact encouraged a search for elliptical instability.

In general, to describe an inertial mode of a thick spherical shell is a challenging problem, but one that must be solved in order to model an elliptical instability with the same geometry. A variety of approximate solutions for inertial modes of a spherical shell have been found by Rieutord (1995), Rieutord and Valdettaro (1997) and Henderson (1996). The latter employed a finite-element method to obtain what are known as 'weak solutions' of the Poincaré problem. In the present work a method is introduced that begins with the numerical solutions of Henderson and proceeds to find the growth rates for certain elliptical instabilities of a thick spherical shell of rotating fluid.

An elliptical instability occurs when a rotating fluid is perturbed so that two inertial modes not only become excited together, but also interact to amplify each other. The amount of growth is limited only by the dissipation, which is due to viscosity and later turbulence. A pair of inertial modes can be denoted by $\lambda_1,(n_1, m_1, k_1)$ and $\lambda_2,(n_2, m_2, k_2)$, where k is the azimuthal wavenumber, n and m are the meridional 'wavenumbers', and λ is the dimensionless

Fig. 1. Bottom view of maximally deformed (fractured) inner boundary.

eigenfrequency. As will be explained further below, an instability of a rotating fluid is possible if $n_1 = n_2$, $k_1 - k_2 = 2$, and $(\lambda_1 - \lambda_2)/2 \approx \omega/\Omega$, where ω/Ω is the angular frequency of the elliptical perturbation divided by that of the basic rotation. It has been shown that the gravest instabilities, which are called subharmonic resonances, each involve the interaction of an inertial wave and its adjoint (Kerswell, 1994). However, the criteria for elliptical instability can also be satisfied by other combinations of inertial modes.

2. Theoretical formulation

Some growth rates for elliptical instabilities in a spheroidal cavity have been calculated by Gledzer and Ponomarev (1992), using a Galerkin method, and by Kerswell (1994). Those growth rates are determined precisely, insofar as the inertial modes of a full spheroid are known analytically. In the case of a thick spherical shell, however, the inertial modes are represented by solutions of the Poincaré problem that, with certain exceptions, are only known numerically. Henderson (1996) has devised a finite-element method to calculate a discrete approximation for the reduced pressure field of any such inertial mode with low enough wavenumbers. We in turn have adopted certain sets of his pressure data to calculate the growth rates of elliptical instabilities in a thick spherical shell of rotating fluid. Further discussion along these lines by Seyed-Mahmoud et al. (1997) is forthcoming. Only those computational results that have been a basis for comparison with our experimental results are presented below.

In order to verify our approach, the elliptical instability associated with the spin-over mode was singled out, then growth rates calculated from the approximate and exact solutions for the velocity field were compared. The frequency of the instability, which we call the spin-over instability, is equal and opposite to the frequency of the rotation, so the velocity field of the disturbance is stationary with respect to a laboratory frame of reference. Hence, we observe a non-rotating but amplifying instability whose dimensionless growth rate is given by:

$$\delta = \pm\sqrt{\frac{\varepsilon^2 V_{1,-1} V_{-1,1}}{N_2^1 N_{-1}^2 - \varepsilon^2 V_{1,-1} V_{-1,1}}} \qquad (1)$$

where:

$$N_k^2 = \int \boldsymbol{u}_k \cdot \boldsymbol{u}_k^* \, d^3\boldsymbol{r}$$

$$V_{kl} = \int T\boldsymbol{u}_l \cdot \boldsymbol{u}_k^* \, d^3\boldsymbol{r}$$

and:

$$T = \begin{pmatrix} \cos 2\phi & -\sin 2\phi & 0 \\ -\sin 2\phi & -\cos 2\phi & 0 \\ 0 & 0 & 0 \end{pmatrix}$$

in a cylindrical coordinate system (r,ϕ,z). Note that ε is defined as the ellipticity of the boundary in an equatorial plane, not a meridional plane. The $\boldsymbol{u}_k$ are obtained directly from the analytical expressions:

$$\boldsymbol{u}_1 = \left(-iz\hat{r} + z\hat{\varphi} + ir\hat{z}\right)e^{i\phi}$$

$$\boldsymbol{u}_{-1} = \left(iz\hat{r} + z\hat{\varphi} - ir\hat{z}\right)ei\phi$$

or indirectly from the numerical pressure field by finite difference methods. The independent calculations of the growth rate were in agreement to three significant digits for ellipticity in the range $\varepsilon \leq 0.25$ approximately. At small ellipticity the relationship $\delta \approx \varepsilon/2$ is satisfied by the growth rate.

The dimensional growth rate $\Omega\delta$ is the property of the instability that becomes relevant in discussion of the experiments and their geophysical applications. Moreover, the growth rate of an elliptical instability must actually be weighed against the decay rate, since a real fluid always involves some dissipation. If the viscous decay rate and inviscid growth rate are equal, the net growth rate is zero and no instability exists. In our experiments, viscous dissipation occurs primarily through boundary layer processes, so the scale for the decay rate is the square root of the Ekman number:

$$E = \upsilon/\Omega R^2$$

where υ is the kinematic viscosity of the fluid, Ω is the angular frequency of the rotation, and R the length scale of the cavity. Accordingly, the net dimensional growth rate of the spin-over instability is approximately:

$$\left(\varepsilon/2 - \alpha\sqrt{E}\right)\Omega \qquad (2)$$

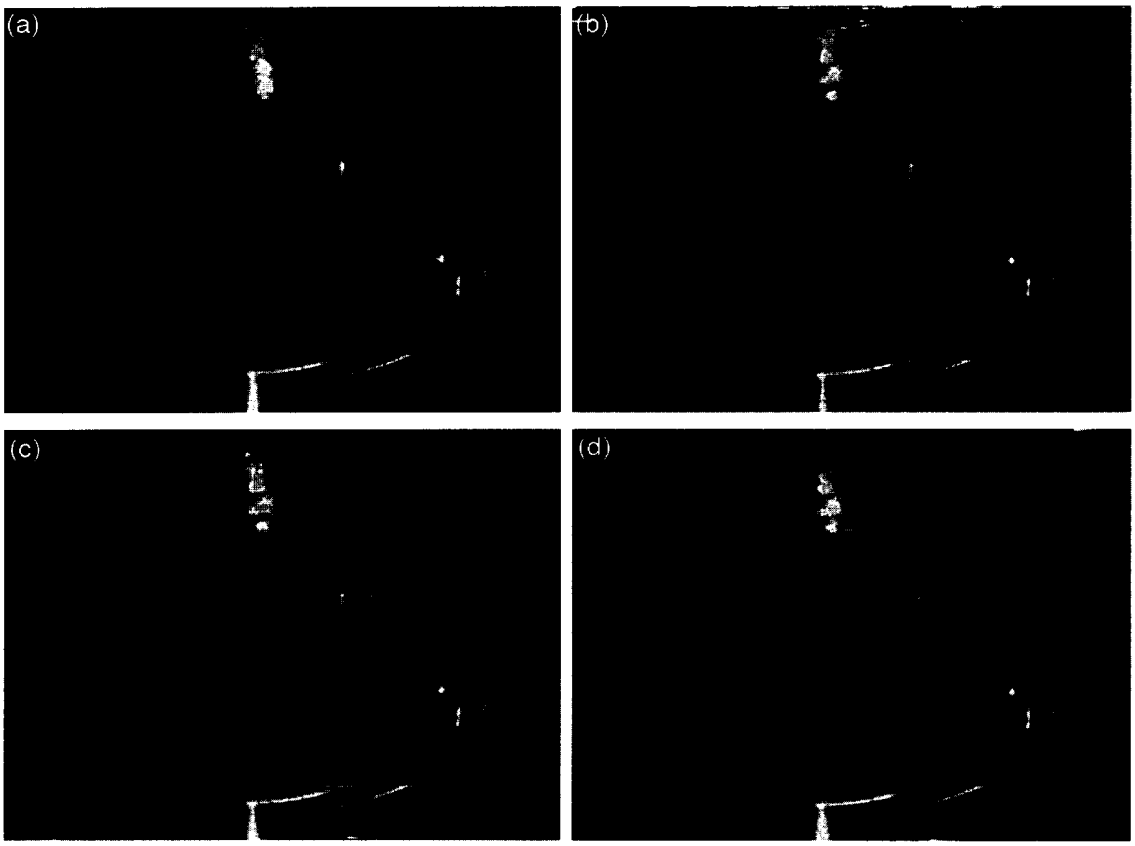

Fig. 2. Linotronic print from VHS video depicting the spin-over instability in the spheroidal shell of fluid.

where $\alpha \approx 1.8$ is the coefficient of the decay rate (Hollerbach and Kerswell, 1995). In our experiments $E = 4.5 \times 10^{-5}$, so the net growth rate of the spin-over instability should be approximately $(\varepsilon/2 - 0.012)\Omega$. Similarly, in geophysical applications E is the Ekman number of the Earth's fluid outer core and ε is the ellipticity of the core–mantle boundary due to tidal forces.

3. Experimental method

The apparatus used to excite the elliptical instability in a spherical shell of rotating fluid was as follows: a rigid outer boundary, with radius $R =$ 10.0cm, was rotated about a fixed vertical axis by a servo-controlled motor that maintained a constant angular frequency to within a 0.15% tolerance. A flexible inner boundary, with mean radius 3.5 cm, was deformed continuously by another servo-controlled motor that drove a rotor arm. The inner boundary was composed of an elasto-plastimer but was lined at the equator with a copper belt in contact with roller bearings at opposite ends of the rotor arm. Because the second motor was mounted on the outer boundary, control of the perturbation was through electrical slip-rings that were coaxial with the rotation. While the rate of rotation was set with respect to the laboratory frame of reference, the rate of perturbation was set with respect to the rotating frame. If the second motor turned the rotor arm in a retrograde sense at the same rate as the first motor rotated the entire shell, the elliptical deformation of the inner boundary would remain stationary with respect to the laboratory frame of reference as the rotating fluid moved past. Fig. 1 shows how the amplitude of the perturbation was adjustable, in the range 0–0.5 cm, by means of a digital thumbwheel (not shown). Although only the inner boundary was deformed, and not precisely into the shape desired, an elliptical instability was nevertheless excited in the rotating fluid.

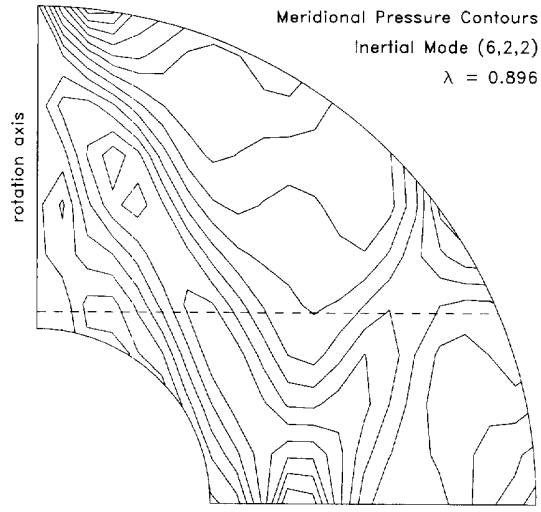

Fig. 3. Calculated pressure contours for the (6,2,2) mode for a spherical shell of rotating fluid. $\lambda = \omega/\Omega = 0.896$. Dashed line is approximate position of laser sheet and corresponds to the plane of the plots given in Figs.6 and 7.

For our experiments the working fluid consisted of distilled water seeded with aluminum flakes, and prior to each run a fresh volume of this suspension was transferred by syphon into the spherical shell. Once the amplitude of the perturbation was set, the motors were started in sequence to drive the rotation and perturbation with periods on the order of 1 s. Initially, the angular velocities of the rotation and perturbation were set equal but opposite, since the fundamental subharmonic resonance was expected to be stationary in the laboratory frame. The response of the rotating fluid to such excitation was observed by two methods.

All quantitative detection of the inertial modes or elliptical instability was by means of Digital Particle Imaging Velocimetry (DPIV, Dantec). With this method the displacements of certain fluid particles are computed by cross-correlating pairs of images taken a few milliseconds apart. In most of our experiments, the digital camera was mounted in the rotating frame of the rigid outer boundary so as to observe the fluid particles that lay in the lateral plane at right angles to the rotation axis and roughly tangent to the lowest point of the inner boundary. This slice of seeded fluid was illuminated by a sheet of light, which was produced by passing a 2 W laser beam (Argon, Coherent Laser) through a cylindrical lens. The displacements measured with the DPIV system were calibrated simply by placing a metric ruler in the plane of observation before the experiment. Pairs of digital images, 512×480 pixels, were taken by a camera (Multicam CCD, Texas Instruments) at intervals of 33 ms and stored in a frame-

grabber board. Subsequently, these images were cross-correlated by the software to obtain the displacement field, and next the velocity field, over a 5 cm × 5 cm square in the illuminated plane.

The growth of an elliptical instability was also observed in a real-time manner by means of an analogue video camera (VHS) that recorded the movement of aluminum flakes under illumination in a meridional plane. When the video was reviewed frame by frame, the elliptical instability was discovered and the image was converted to hard copy by a Linotronic printer.

4. Results

Direct observation of what we have identified as the elliptical instability is shown in the collection of four plates of Fig. 2. These images are Linotronic prints from a VHS video of the laser illuminated meridional plane. The black rectangle in each plate covers an incorrect date which added nothing to the image and obscured the view of the fluid. For this set of images the ellipticity of the inner boundary, $\varepsilon = 0.041$, rotation speed $\Omega = 5.24$ rad/s, and the perturbation speed, $\omega = 4.90$ rad/s. This condition for instability corresponds to a slow drift of the instability in the direction of rotation as seen from the laboratory reference frame and was found by searching in rotation near the condition $\Omega \approx \omega$, since the theoretical location of the spin-over instability for a spheroid would occur for rotation speed equal and opposite to the perturbation speed. The ellipticity ε was sufficiently larger than 2×0.012, the scale of the dissipation rate, so that we would excite the instability, but small enough so as not to fracture the elasto-plastimer.

The sequence of events leading to the onset of the

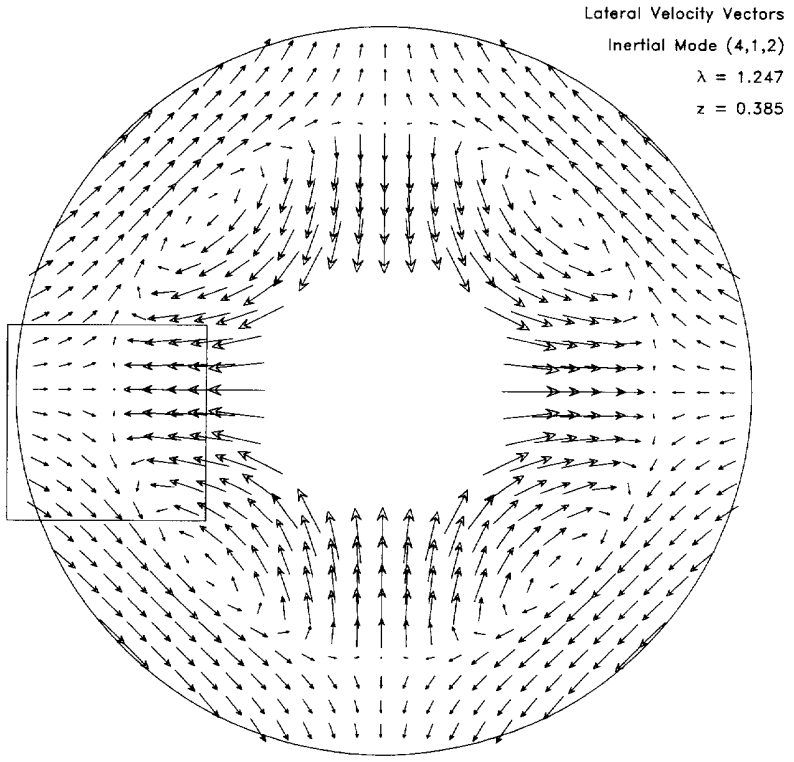

Fig. 4. Calculated velocity vectors for the mode (4,1,2) in a plane perpendicular to the rotation axis approximately tangent to the inner sphere. $\lambda = \omega/\Omega = 1.247$.

instability is as follows. The laser sheet illuminated the sphere and the rotation of the container was started while the video was recording. After solid body rotation was established for the spheroidal shell of fluid, the perturbation was switched on. About 30 s later, violent motion was observed near the axis of rotation, as can be seen in (a) for the fluid columns directly underneath the inner sphere. Subsequently what appear to be characteristic lines can be observed radiating up to the right at about 35° to the vertical in (b) and (c) while large amplitude of the columns underneath and to the right of the inner sphere can be seen beginning to develop in (d).

The experiment was repeated several times to estimate the growth rate of the instability by measuring the time interval between the start-up of the perturbation and the onset of the instability as observed in Fig. 2. The growth rate observed was 0.031 s^{-1} which is comparable to the predicted rate $(0.041/2 - 0.012) \times 5.24 = 0.045\ s^{-1}$.

The setting of the rotation speed was reduced by about 3% to $\Omega = 5.08$ rad/s and the experiment was repeated. No evidence of instability was observed.

If they exist, wavenumber 2 inertial modes will be excited in our spheroidal shell of rotating fluid by the flexible inner boundary if two conditions are met. First, the mode must have a velocity field which is sufficiently well coupled to the velocity of the flexible surface which is perturbing the fluid. Second, the frequency ratio ω/Ω must be sufficiently close to the actual eigenfrequency λ of the mode to be excited. It is important to note, however, that even if these two conditions are met and a mode is excited, observation of the mode may be obscured by the development of an elliptical instability.

To satisfy the first condition, only low order modes, symmetrical about the equator with azimuthal wavenumber 2, need be considered. Two modes which satisfy this condition are the (4,1,2) and the (6,2,2) modes. The properties of these modes

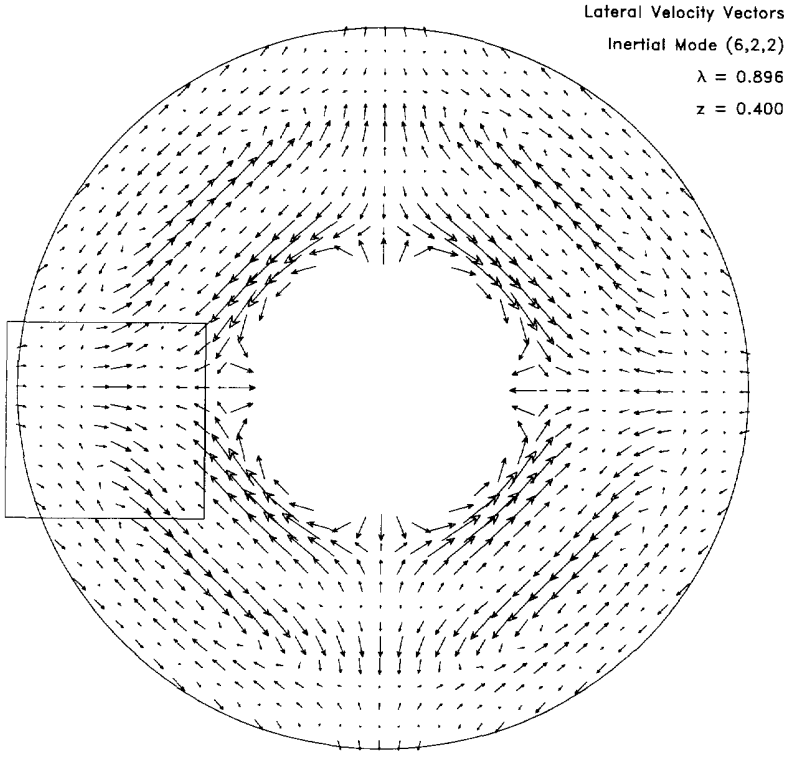

Fig. 5. Calculated velocity vectors for the mode (6,2,2) in a plane perpendicular to the rotation axis approximately tangent to the inner sphere. $\lambda = \omega/\Omega = 0.896$.

were found using the finite-element method developed by Henderson (1996) and are displayed below in two different planes. First, a mode identified as (6,2,2) with computed eigenvalue $\omega/\Omega = 0.896$ is depicted in Fig. 3 which is a plot of pressure contours in the meridional plane. This mode is noteworthy not only because it satisfies the conditions for excitation as stated above, but also because it clearly displays the significant role of the characteristic surfaces which form a 'V' pattern emanating from the equator just to the right of the inner sphere. It is also noteworthy that distortion of the characteristic surfaces referred to above in (b), (c) and (d) of the Linotronic prints of Fig. 2 were important markers in observing the onset of the instability. Indeed the slopes of these characteristics are similar for the two different modes in Fig. 2 and Fig. 3 because it is the ratio ω/Ω which fixes these slopes.

In the second view, plots of the velocity field of the (4,1,2) and (6,2,2) modes in a plane perpendicular to the axis of rotation and approximately tangent to the inner sphere are shown in Figs. 4 and 5 respectively. It is this plane which is illuminated by the sheet of laser light used to obtain the DPIV results. The area of observation is a square approximately 5 cm × 5 cm while the images of the expected velocity fields for a pure mode are about 9.3 cm in radius, because they correspond to a cut at about 3.5 cm below the centre of the 10 cm radius sphere. Accordingly the DPIV square of observation corresponds to a little more than one-half of the radius of the circle in Figs. 4 and 5.

Velocity vectors from the DPIV images corresponding to the experimental case $\omega/\Omega = 1.260$ are shown in Fig. 6 and can be compared to a 5 cm × 5 cm window of Fig. 4 near the equator and roughly central between the circumference and the circular boundary. In the case shown the phase of the ob-

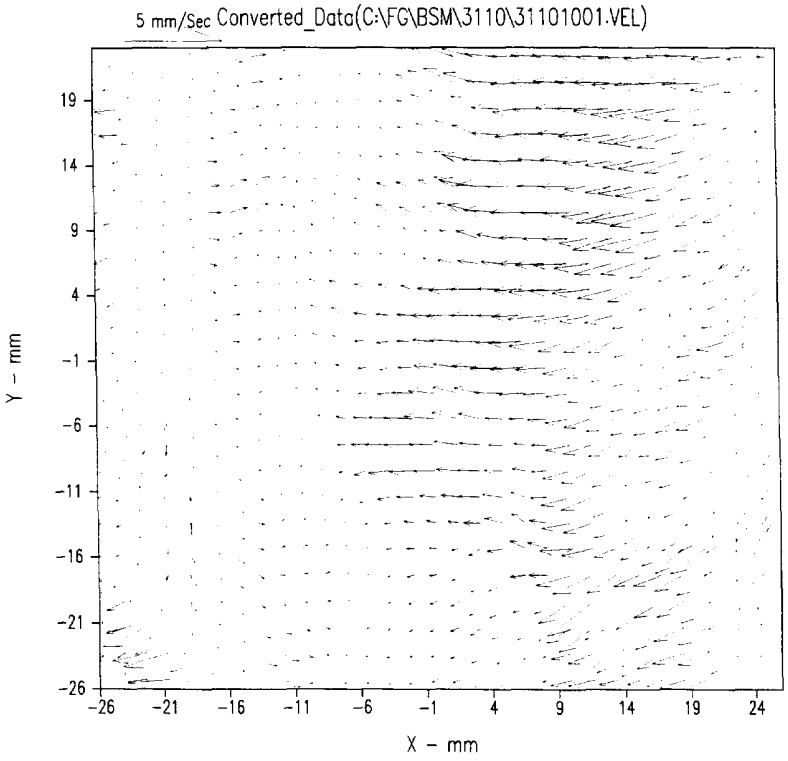

Fig. 6. Velocity vectors obtained from experimental observations in the plane perpendicular to the rotation axis and tangent to the inner sphere. Settings are $\omega = 4.155\ s^{-1}$, $\Omega = 3.261\ s^{-1}$, $\omega/\Omega = 1.260$.

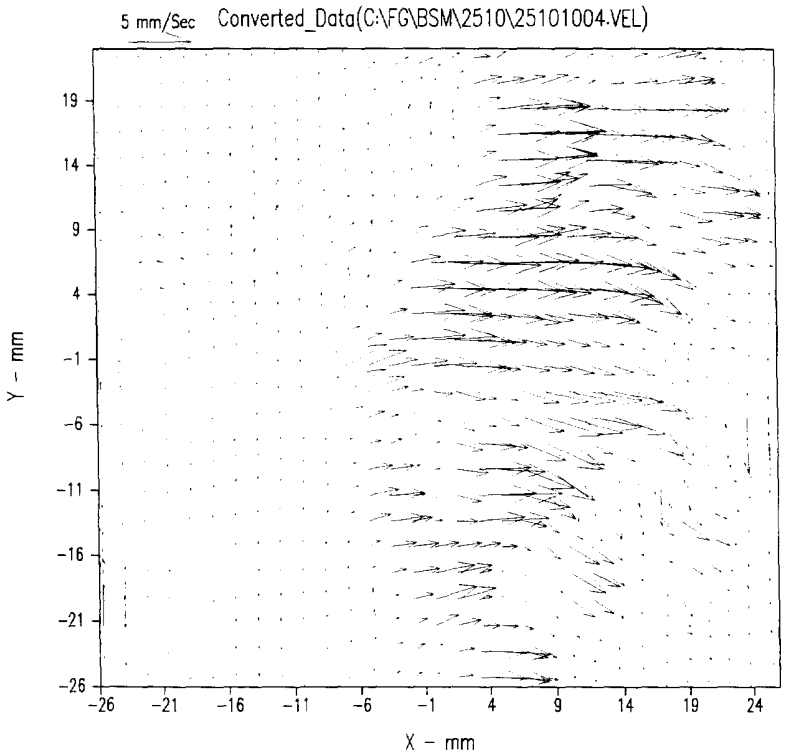

Fig. 7. Velocity vectors obtained from experimental observations in the plane perpendicular to the rotation axis and tangent to the inner sphere. Settings are $\omega = 2.482\ s^{-1}$, $\Omega = 2.796\ s^{-1}$, $\omega/\Omega = 0.887$.

served flow is very close to the phase of the calculated flow in Fig. 4. It should be remembered, of course, that the observed flow is not exactly at resonance so that there will be other components due to neighbouring modes in the DPIV result.

Shown in Fig. 7 are the velocity vectors for what has been tentatively identified as the (6,2,2) mode depicted in Fig. 5. In this DPIV result there is more interference from other modes than in the case of Fig. 6. It is noteworthy that significantly decreased response of the fluid to the elliptical perturbation takes place when the ratio ω/Ω is changed from the values reported here.

Detailed plots of velocity fields from DPIV will make it possible to measure the onset of the elliptical instability in future experiments. It will be possible to follow the development of the instability as it grows, since a sequence of image pairs can be obtained over time. Since the control of the rotation is done through servo-controllers, experiments can be repeated precisely to build an arbitrarily long set of detailed velocity images.

5. Discussion

The experimental results presented here confirm the existence of the elliptical instability in a rotating spheroidal shell of fluid. We have tentatively identified the instability observed with the spin-over instability, as confirmed by growth rates and frequency, which are close to those expected from the theory developed here. While the calculated growth rates presented here for the spin-over instability correspond to a perturbation which is fixed in inertial space, ongoing theoretical work for a non-stationary perturbation indicates that growth rates achieve a maximum value when there is a small departure from stationarity (Seyed-Mahmoud et al., 1997). This theoretical development has used the approximate

pressure field from a finite-element method to solve the instability problem for a rotating spheroidal shell of fluid. Other modes of instability can now be found using this method and compared to experimental results.

The existence of wavenumber 2 inertial modes has been confirmed experimentally for a thick rotating spheroidal shell of fluid. Thus instabilities due to interaction between modes with wavenumber 0 and 2 can exist in the shell as well as the ± 1 pair of spin-over modes observed in the present experiment.

We consider here the possibility that tidal excitation of the core–mantle boundary near semi-diurnal periods could excite an elliptical instability in the Earth's fluid outer core. Although many instabilities are possible, we consider the growth of the spin-over instability that we have observed in our experiments. If we consider only viscous dissipation, the actual growth rate of this instability of the core would be approximately that given by Eq. (2) above. If we first ignore dissipation and set $\varepsilon = 5 \times 10^{-8}$, corresponding to a semi-diurnal tidal distortion of the core–mantle boundary, the growth period is about 7000 years. If, however, $\sqrt{E}$ is sufficiently close to $\varepsilon/2$, the actual growth period becomes greatly extended. For example at $E \approx 0.3 \times 10^{15}$, the time taken for elliptical instability to develop becomes 10^6 years, a geomagnetic time scale. As pointed out by Kerswell (1994), the electromagnetic dissipation is comparable to the mechanical dissipation, so the role of the elliptical instability in the dynamics of the core and hence dynamo theory is likely important. If a reversal of the geomagnetic field could be identified with a particular instability, the lifetime of the field in a particular polarity could then be used to estimate the dissipation rate for the core and hence provide a limit on viscosity and conductivity as determined by the model used for dissipation.

Acknowledgements

We are grateful to Richard Kerswell and an anonymous referee for their valuable suggestions which helped us clarify and improve the presentation of this work.

References

Aldridge, K.D., 1975. Inertial waves and the Earth's outer core. Geophys. J. R. Astr. Soc. 42, 337–345.

Gledzer, E.B., Ponomarev, V.M., 1992. Instability of bounded flows with elliptical streamlines. J. Fluid Mech. 240, 1–30.

Henderson, G.A., 1996. A finite-element method for weak solutions of the Poincaré problem. PhD Thesis, York University, Toronto, Canada.

Hollerbach, R., Kerswell, R.R., 1995. Oscillatory internal shear layers in rotating and precessing flows. J. Fluid Mech. 298, 327–339.

Kerswell, R.R., 1993. The instability of precessing flow. Geophys. Astrophys. Fluid Dyn. 72, 107–144.

Kerswell, R.R., 1994. Tidal excitation of hydromagnetic waves and their damping in the Earth. J. Fluid Mech. 274, 219–241.

Lumb, L.I., Aldridge, K.D., 1988. An experimental study of inertial waves in a rotating spheroidal shell of fluid. In: Smylie, D.E., Hide, R. (Eds.), Structure and Dynamics of the Earth's Deep Interior, pp. 35–39. American Geophysical Union.

Lumb, L.I., Aldridge, K.D., Henderson, G.A., 1993. A generalized core resonance phenomenon: inferences from a Poincaré model. In: Le Moüel, J.L., Smylie, D.E., Herring, T.A. (Eds.), Dynamics of the Earth's Deep Interior and Earth Rotation, Geophysical Monograph 72, IUGG Vol. 12, pp. 51–68. American Geophysical Union.

Malkus, W.V.R., 1989. An experimental study of global instabilities due to the tidal (elliptical) distortion of a rotating elastic cylinder. Geophys. Astrophys. Fluid Dyn. 48, 123–134.

Manasseh, R., 1992. Breakdown regimes of inertia waves in a precessing cylinder. J. Fluid Mech. 243, 261–296.

Manasseh, R., 1994. Distortions of inertia waves in a precessing cylinder forced near its fundamental mode resonance. J. Fluid Mech. 265, 345–370.

McEwan, A., 1970. Inertial oscillations in a rotating fluid cylinder. J. Fluid Mech. 40, 603–640.

Rieutord, M., 1995. Inertial modes in the liquid core of the Earth. Phys. Earth Planet. Int. 91, 41–46.

Rieutord, M., Valdettaro, L., 1997. Inertial waves in a rotating spherical shell. J. Fluid Mech. 341, 77–99.

Seyed-Mahmoud, B., Henderson, G.A., Aldridge, K.D., 1997. Elliptical instability in rotating ellipsoidal fluid shells in preparation.

Stergiopoulos, S., Aldridge, K.D., 1984. Ringdown of inertial oscillations in a spheroidal shell of rotating fluid. Phys. Earth Planet. Int. 36, 17–26.

Thompson, R., 1970. Diurnal tides and shear instabilities in a rotating cylinder. J. Fluid Mech. 40, 737–751.

Vanyo, J., Wilde, P., Cardin, P., Olson, P., 1995. Experiments on precessing flows in the Earth's liquid core. Geophys. J. Int. 121, 136–142.

Vladimirov, V.A., Tarasov, V.F., 1985. Resonant instability of the flows with closed streamlines. In: Kozlov, V.V. (Ed.), Laminar–Turbulent Transition, Springer-Verlag, pp. 717–722.